Acta Geotechnica (2025) 20:3905–3927
https://doi.org/10.1007/s11440-025-02608-9

RESEARCH PAPER

Experimental investigation and image-based analysis of clay slurry consolidation with prefabricated horizontal drain

Peng-Lin Li[1] · Zhen-Yu Yin[1,2] · Ding-Bao Song[1] · Jian-Hua Yin[1]

Received: 2 September 2024 / Accepted: 9 March 2025 / Published online: 11 April 2025

Abstract

The characteristics of the consolidation facilitated by prefabricated horizontal drains (PHDs) combined with vacuum loading, and the evolution of the soil column surrounding the PHDs, which significantly affects the acceleration efficiency, remain insufficiently understood. This study conducts experimental investigations into PHD-assisted consolidation, employing an enhanced digital image correlation (DIC) technique. A novel texture seeding method for slurry, essential for DIC measurements, was developed and applied to consolidation model tests with varying PHD pave rates. Data on vacuum-discharged water reveal that the consolidation rate increases with the pave rate, albeit non-linearly. The DIC-observed plane strain fields exhibit distinct non-uniform features, with zones closer to the PHD consolidating significantly faster than other regions. The shape of the soil column observed through the DIC method is approximately elliptical, and its dimensions are characterized using empirical equations, highlighting the feasibility of optimizing PHD spacing in engineering design. The void ratio distribution was derived from strain information, validating the findings related to the soil column. Additionally, excess pore pressure distributions suggest that the effective range of vacuum transfer lies between 20 and 30 cm. Water content and undrained shear strength distributions provide key insights into the non-uniformity of PHD-improved consolidation. Further studies are recommended to quantify the optimal pave rate and the effective transfer distances of vacuum pressure and incorporate the observed soil column information into PHD-assisted consolidation analysis.

Keywords Clay slurry consolidation · Digital image correlations · Prefabricated horizontal drain · Vacuum loading

1 Introduction

Prefabricated horizontal drains (PHD) have been proposed and successfully applied in engineering to treat dredged slurry [4, 10, 15, 19, 23, 43]. The approach offers several advantages. It integrates blow filling and vacuum reinforcement, improving processing efficiency. The self-sealing property of high-water-content soil eliminates the need for additional sealing measures, thereby reducing costs. Moreover, this method can avoid installation challenges in low-strength slurry and prevent bending issues. Additionally, the consolidation rate is enhanced by reducing the soil layer thickness between PHDs, which shortens the drainage path.

Different numerical methods have been developed to analyze the PHD-assisted consolidation. Nogami and Li [20] performed the consolidation modeling of layered clay with horizontal and vertical drains, providing a design method for an optimum drainage system. Nagahara et al.

✉ Zhen-Yu Yin
zhenyu.yin@polyu.edu.hk

Peng-Lin Li
pengl.li@connect.polyu.hk

Ding-Bao Song
dingbao.song@polyu.edu.hk

Jian-Hua Yin
jian-hua.yin@polyu.edu.hk

[1] Department of Civil and Environmental Engineering, The Hong Kong Polytechnic University, Hung Hom, Kowloon, Hong Kong, China

[2] Research Centre for Resources Engineering Towards Carbon Neutrality (RCRE), The Hong Kong Polytechnic University, Hung Hom, Kowloon, Hong Kong, China

[19] conducted a finite element analysis and validated the simulations with field test data of a fill treated by PHDs in Noto Airport. Chai et al. [5] proposed a unit cell-based method for analyzing PHD-improved soil consolidation. Menon and Bhasi [18] analyzed the influence of the PHD-assisted method on various soil types. Song et al. [24, 25] developed a large strain consolidation model using a piecewise approach for soft soils with PHDs. Zhang et al. [44] and Sun et al. [32] derived plane strain consolidation solutions using the finite difference method, validating their models with laboratory and field tests. Chai et al. [6] introduced a method with explicit equations considering nonlinear mechanical and geometrical characteristics in PHD-accelerated consolidation. Pan and Li [21] further introduced the influence of the stacking process on the PHD-assisted consolidation. A new simple method [9] and analytical solution [26] for PHD-assisted consolidation modeling were also developed. These studies demonstrate the effectiveness of treating very soft soils using PHD. However, most validation data report only soil surface settlement (vertical strain), which inadequately represents the inherently two-dimensional (2D) nature of PHD-improved consolidation. Moreover, soil column formation near the drain board often limits the acceleration effect in zones further away [36, 37, 41, 48]. The soil column is a dense zone with low water content and low hydraulic conductivity [11]. Understanding the 2D displacement profile is crucial for studying the formation mechanism of soil columns. Several tests have been conducted to investigate the PHD-assisted consolidation behavior of clayey soils. Khachan and Bhatia [14] applied a small centrifuge to observe the dewatering process. Song et al. [25] performed PHD-assisted model tests with stage filling, simulating engineering practices. Zhang et al. [45] reported laboratory tests with different PHD pave rates and height-to-width ratios to analyze the factors affecting the PHD-improved efficiency. Wu et al. [39] conducted four indoor model tests with PHDs to analyze the influence of surcharge loading rate on the consolidation process. Zhou et al. [50] investigated the membrane-free horizontal vacuum method for accelerating consolidation. Experimental investigations on dewatering dredged slurry treated by PHDs-PVDs were also carried out recently [17, 42]. Among these tests, only Wu et al. [39] measured the horizontal displacement after soil excavation at the end of the test. However, detailed data on 2D displacement profiles throughout the PHD-assisted consolidation process remain unavailable.

The digital image correlation (DIC) technique has recently been applied in geotechnical engineering to observe the displacement field. This advancement is enabled by advancements in image-capturing technology and analysis methods. Unlike traditional methods, such as using a dial gauge or linear variable differential transformer (LVDT) which measures displacement only at fixed points, the DIC method allows non-contact measurement of the entire displacement profile in the observed area. White et al. [38] pioneered a deformation measurement system using image analysis. This method effectively captured the 2D displacement field of sand and low-water-content clayey soils [7, 27–29, 33, 34, 47]. Clayey soils lack the natural textures necessary for image analysis, so artificial textures are required. Stainer and White [27] emphasized the importance of texture and detailed methods to create and optimize it. The seeding method is to put the dyed sand on the observed zone, producing distinct textures due to color contrast between the test soil and dyed sand. Many researchers [7, 28, 47] have since adopted this method in model tests to study clayey soils with low water content. Most applications have focused on sand with natural textures [1, 38] or clayey soils with low water content [7, 22, 28, 47], where artificial textures are easier to create.

Many researchers [3, 12, 30, 31, 49] have applied the DIC technique to observe the PVD-assisted consolidation of soils with water content above the liquid limit. Cai [3] and Zhou et al. [49] analyzed the displacement profiles around PVDs under vacuum loading to study soil column formation. Sun et al. [32] adopted the DIC technique to investigate the soil column characteristics and proposed two methods to estimate the evolution of soil column dimensions. He et al. [12] performed model tests to examine the effect of initial water content on soil column formation. However, these studies only reported the evolution of soil column in one direction and did not reveal its full shape. The artificial texture creation methods used in these studies relied on traditional seeding techniques, such as sprinkling dry quartz or carbon powder on the observation window, which are better suited for clayey soils with low water content. For very soft soils, these methods have limitations, including detachment due to soil shrinkage, uneven powder distribution, and disturbances due to model installation. Thus, an improved artificial seeding method is needed for conducting image analysis on very soft soils.

This study aims to explore the non-uniform deformation behavior of the PHD-assisted consolidation process with vacuum loading using an enhanced image analysis method. The novelty of the research lies in the development of an enhanced artificial seeding method for clayey soil with high water content. The proposed seeding method is introduced to capture the 2D displacement field, offering new insights into soil column formation and non-uniform deformation characteristics under different pave rates. Key parameters, including discharged water mass, discharge rate, excess pore water pressure, water content, and

undrained shear strength, were also monitored and discussed.

2 Experimental programs

2.1 Test material

The Hong Kong Marine Deposit (HKMD) collected from Lantau Island in Hong Kong was used in the PHD-improved consolidation model tests. The physical properties are listed in Table 1. An oedometer test starting from a very small stress of 0.025 kPa was conducted on HKMD with an initial water content of 197.7%. The oedometer test is conducted using a novel apparatus, capable of applying minimum stress of 0.025 kPa to clay slurry with a water content exceeding 8 LL suitable for clay slurry [16]. The consolidation parameters are provided in the supplementary file. Figure 1 illustrates the particle size distribution of the HKMD. Detailed information on the test soils is provided to facilitate potential numerical modeling or comparative analysis with similar experiments by other researchers. The PHD used in the test features a filter fixed on the core, creating an individual drainage channel for each core. It is a novel anti-clogging drain board, with a thickness of 4 mm and a width of 100 mm. The PHD has a discharge capacity exceeding 50 cm^3/s.

2.2 Model setup

The presented model system, as illustrated in Fig. 2, consists of a cuboid plexiglass model tank with inner dimensions of 500 mm × 150 mm × 600 mm (length × width × height). A prefabricated drain board is positioned in the center of the model tank bottom. An air–water separation bottle with an electronic scale measures the mass of the drained water resulting from vacuum loading. An image-capturing system includes a 16-million-pixel industrial camera (4912 × 3684 pixels), a fixed camera bracket, LED studio lighting, and a computer for image storage. The size of the model tank was chosen according to the general horizontal and vertical spacings

Table 1 Basic physical properties of HKMD

Properties	Value
Specific gravity, G_s	2.62
Liquid limit, LL (%)	49
Plastic limit, PL (%)	31
Plastic index, PI (%)	18

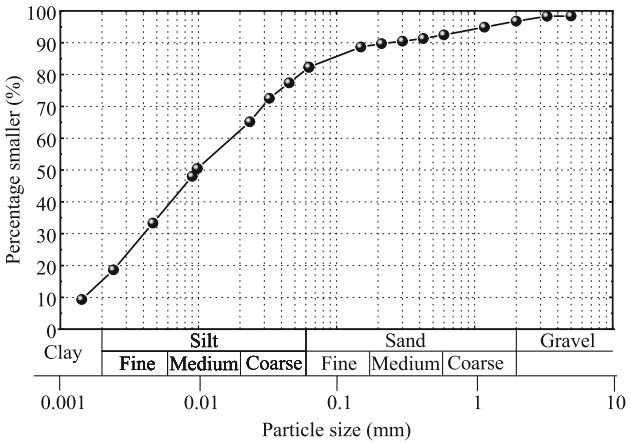

Fig. 1 Particle size distribution of HKMD

(e.g., 0.5–0.8 m) between the PHDs in engineering practice [23, 43]. The principle is that the practical spacing between the PHDs can be realized by adjusting the width of the PHD since the size of the model tank is not convenient to change. The industrial camera, positioned in front of the observation window, is connected to a platform for setting image resolution and acquisition intervals. With a frame rate of 12 fps, the camera captures up to 12 photographs per second. Stable lighting is ensured using LED lights in a professional studio surrounding the tank. The surroundings and bottom of the model tank were coated with petroleum jelly to reduce friction.

Pore water pressure sensors, with a measurement range from − 100 kPa to 100 kPa and a precision of 0.1 kPa, were fixed on the back of the model tank through threads, as shown in Fig. 2b. A denser distribution of pore water pressure transducers (PPTs) was intentionally positioned in the region closer to the PHD, where more significant changes in pore water pressure were expected compared to the area farther from the PHD. Hand-held vane testers were used to measure the undrained shear strength (S_u) of treated HKMD after the tests. The procedure involved slowly pressing the cross plate head vertically into the soil to be tested. The torque meter handle was then rotated clockwise at a uniform rate until the soil sheared and broke. The undrained shear strength was determined by reading the torque meter scale at this point. The water content was measured by drying method on the soil samples taken from the model test after the test.

2.3 Test procedures

Generating the artificial texture is necessary for image analysis of clayey soils without obvious texture. As employed by the previous studies, the conventional approach for making texture is sprinkling quartz or carbon powder on a petroleum jelly-coated observation window

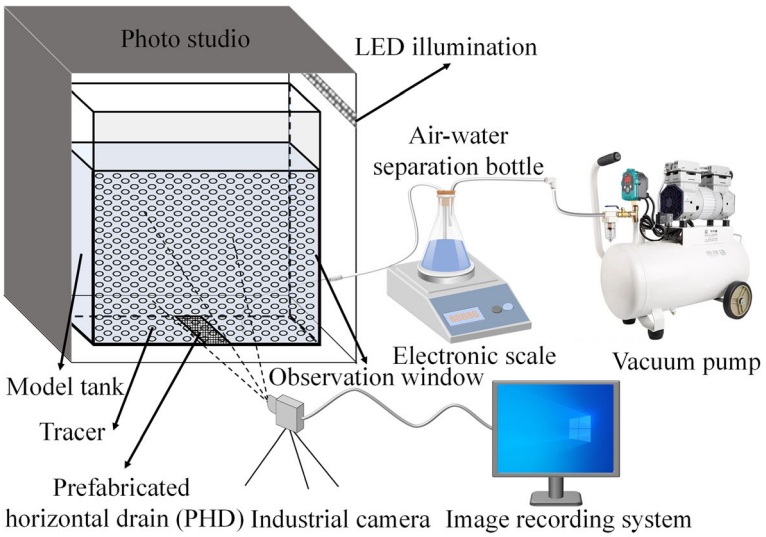

(a)

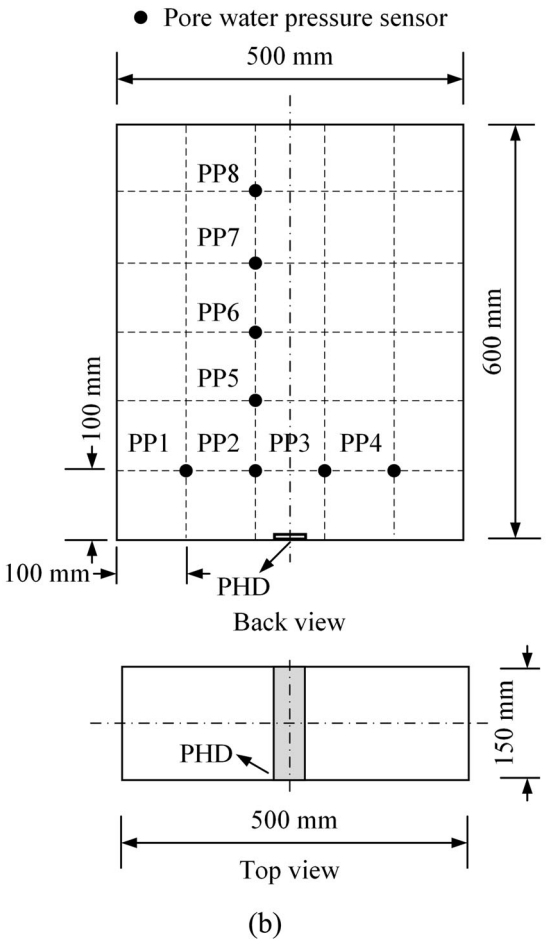

(b)

Fig. 2 Physical model setup: **a** schematic drawing and **b** sensor arrangement behind the model tank and PHD position at the bottom

directly. Nonetheless, this approach faces challenges when applied to high-water-content clayey soil model tests. Primarily, achieving a uniform distribution of quartz powder on the observation window by sprinkling is difficult, particularly in larger model tanks. Additionally, the weak bond between dry quartz or carbon powder and the viewing

window via petroleum jelly is easy to cause tracers to fall off during the model tank installation process. Wu et al. [40] also observed quartz detachment from the soil due to volume shrinkage due to vacuum loading. Collectively, these factors—uneven quartz powder distribution, loss of quartz powder because of installation interference, and detachment due to volume shrinkage—compromise image analysis accuracy. Consequently, an improved texture seeding methodology is required for the investigation of displacement fields for clayey soils with high water content.

To overcome the shortcomings of the traditional seeding method, this study proposes an optimized artificial seeding method suitable for clayey soils with high water content. With the detailed seeding procedure, the model test steps are as follows:

(a) Made a thin and porous plate.

A thin, rigid plate (e.g., acrylic or silicone grease) less than 5 mm thick was used based on the size of the target viewing area. The plate was processed using laser cutting or mechanical methods, such as engraving, to create holes. The distribution patterns of holes can be uniform, quincunx, or random (Fig. 3). The quincunx pattern was preferred for consolidation model tests due to its optimized seeding ratio, which minimizes image analysis errors [27]. This pattern also prevents tracer overlap, a common issue with random distributions as tracers settle with the soil.

(b) Prepared suitable material for seeding texture.

The color and size of the texture material are crucial for making a suitable texture for slurry. A greater color contrast between the texture material and the test soil improves accuracy [27]. Black materials like carbon powder or black-dyed quartz powder are suitable for white soils such as Kaolin clay. Sun et al. [32] and Zhou et al. [49] have used white quartz powder and black carbon powder for this purpose. White quartz powder is preferred because it can be dyed to match the soil color, enhancing image analysis accuracy. The size of the texture material can be determined based on the D_{50} of the test soil as proposed by Cai [3], to minimize interference with the test soil and reduce displacement difference. In this study, a slightly flowable state mixture (Fig. 4b) of white dry quartz powder and water instead of dry quartz powder was adopted in the proposed new texture-making method. The slightly flowable combination of dry quartz powder and water represents an optimal state, facilitating smooth and uniform spreading across the observation window using a brush. The water content in the slightly flowable mixture must be carefully controlled to avoid forming droplet-like balls when brushed onto the observation window. Such droplet-like formations tend to shrink significantly upon water loss, leading to lower-quality textures that adversely affect the accuracy of image analysis.

(c) Scribbled a thin layer of petroleum jelly on the viewing window (Fig. 4c).

The petroleum jelly was used to reduce the friction between the model tank and soil/tracers.

(d) Brushed the flowable mixture on the observing window using a soft brush (Fig. 4d).

In this step, every hole of the porous plate was ensured full of the mixture. Once there was no apparent free water, the porous plate can be carefully removed. Then, the mixture on the observation window was left to dry for 1–2 h. This process allowed the quartz to adhere firmly to the observation window (see Fig. 4e). This method enhanced the bond between the model tank and the soil, minimizing interference due to model installation and allowing the tracer to function optimally.

(e) Stirred the slurry to the target water content and poured it into the model tank (Fig. 4f).

To prevent slurry splashes from contaminating the quartz on the observation window, a thin plastic tremie

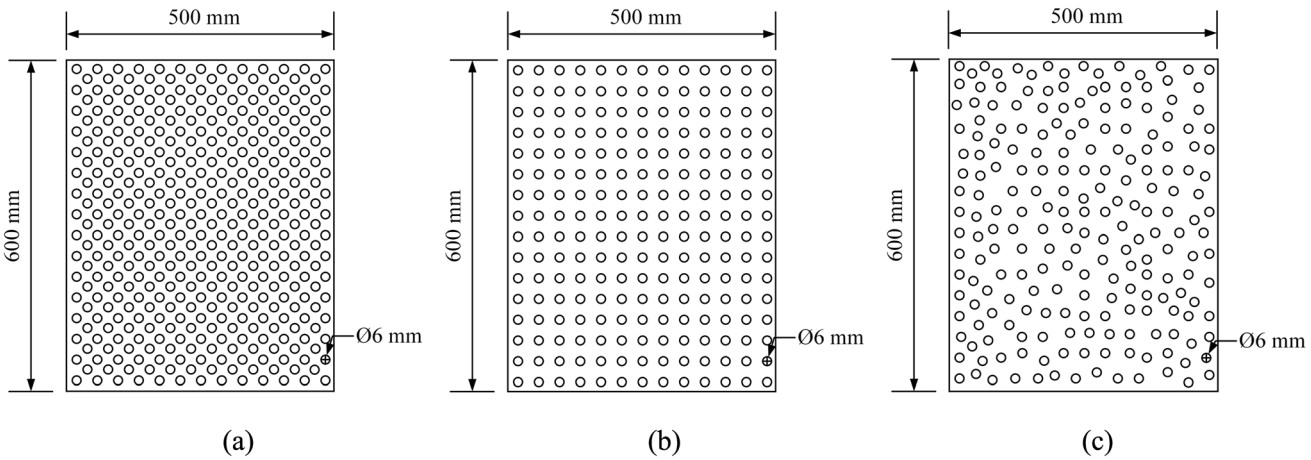

Fig. 3 Hole distribution patterns: **a** uniform distribution, **b** quincunx distribution, and **c** random distribution

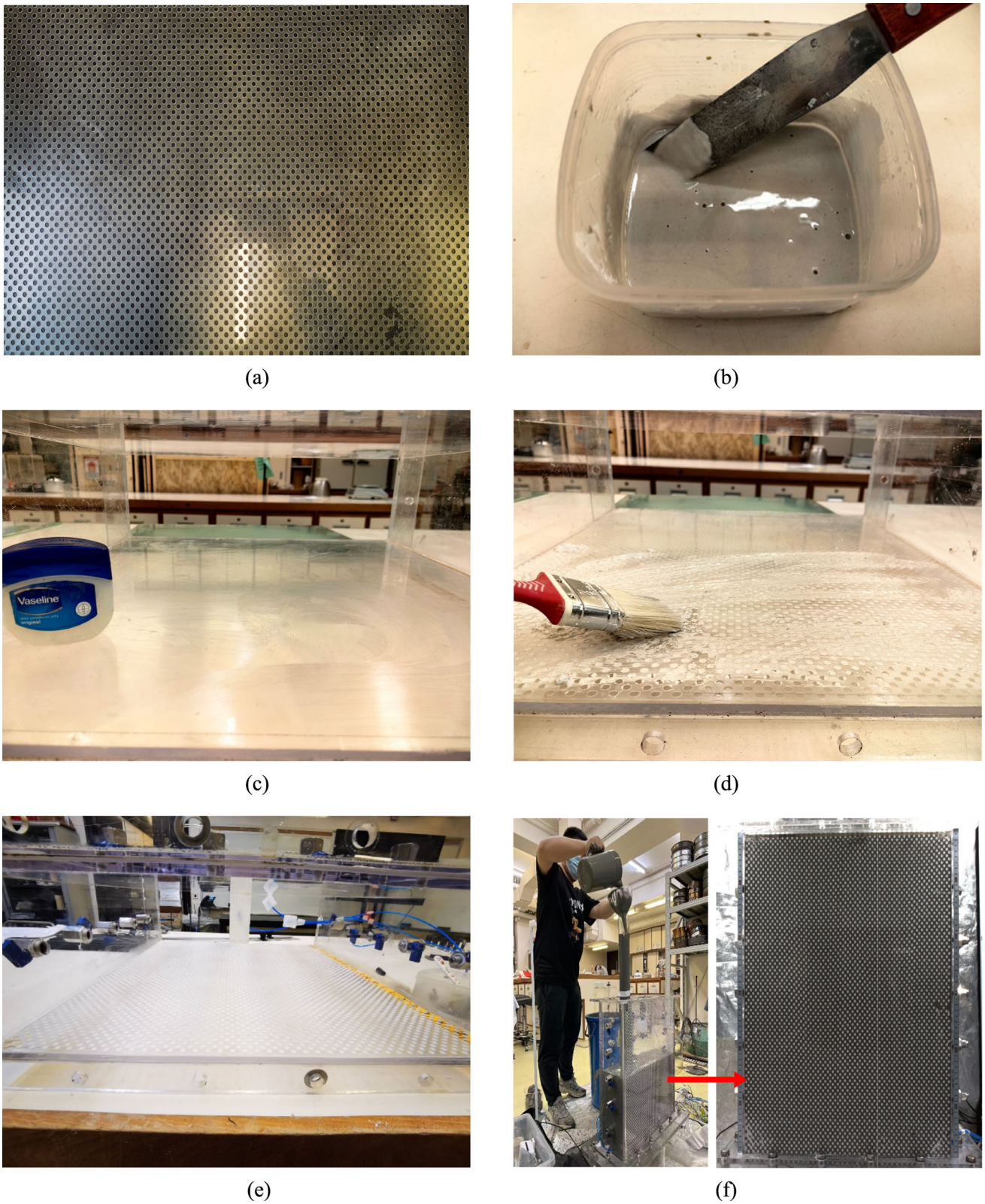

Fig. 4 Setup steps of physical model: **a** prepared a porous acrylic plate, **b** mixed the quart powder with water, **c** coated with a thin layer of petroleum jelly, **d** brushed wet quartz powder, **e** air-dried the quartz, and **f** poured the slurry into the model box

pipe with a diameter of about 100 mm and a wall thickness of 3 mm was used for pouring the slurry. Larger pipe diameters facilitated faster pouring and reduced clogging. The thin wall minimized disturbance during pipe extraction after pouring. When the slurry was poured into the model tank, the dry mixture on the observing window would be soaked and blended with the slurry so that it could settle together with the slurry. This ensured a clear and stable texture on the window, as shown in Fig. 4f, with no quartz shedding after the process.

This approach enables the customization of the texture to meet specific requirements, such as model size, while ensuring its long-term stability and clarity and effectively minimizing potential disturbances caused by model installation. Achieving these characteristics is challenging when using the traditional seeding method in clay slurry.

2.4 Test scheme design

To explore the PHD-assisted plane strain consolidation characteristics of clayey soils with high water contents, three physical model tests with different pave rates, the ratio of drain plate area over total surface area (e.g., bottom area of the model tank in this study) [8, 32], were conducted. Pave rate is a significant factor affecting the performance of PHD. Appropriate pave rate can maintain a good accelerated effect while reducing the use of drain boards and thereby reducing soil treatment costs. The pave rates of three physical model tests were 20% (100 mm/500 mm) for Physical Model 1 (PM1), 15% (75 mm/500 mm) for Physical Model 2 (PM2), and 10% (50 mm/500 mm) for Physical Model 3 (PM3), respectively, achieved by changing the width of PHD due to fixed tank dimensions. The PHD was centrally positioned at the tank bottom, as shown in Fig. 2b. The initial water content of the three model tests is set at 200%, about 4 times the liquid limit of the HKMD. The initial height of the slurry in each test is 600 mm, consistent with typical vertical PHD spacing in engineering practice. In each test, a one-day self-weight consolidation occurred, and then, a vacuum pressure of − 80 kPa in PHD was set to discharge the pore water in the soil. It should be noted that the period of self-weight consolidation has no unified criteria and can be less or longer than one day.

3 Results and discussions

3.1 Discharged water and the drainage rate under different pave rates

Figure 5 shows the mass of the discharged water and the drainage rate of three PM tests. Discharged water mass and drainage rate are intuitive variables reflecting the accelerated consolidation effect of PHD with vacuum pressure. Drainage rate is determined by the slope of discharge water mass with time over smaller time intervals. The experimental results indicate that the mass of discharged water increases with the pave rate. PM1, with the largest pave rate, has the most noticeable effect on discharging the pore water. However, the mass difference of discharged water between PM2 and PM3 is small. The discharged water mass of PM2 is only 100 g higher than that of PM3 after 30 days of vacuum pressure loading. The phenomenon can be explained by the drainage rate as shown in Fig. 5c. The water discharge rate is very high at the beginning of the vacuum application (e.g., 520 g/h for PM1, 440 g/h for PM2, and 370 g/h for PM3). However, a large drainage rate can only be maintained for a short period of only a few hours, followed by a rapid decline before eventually stabilizing. The drainage velocities stabilized at 10 g/h for PM1, 9 g/h for PM2, and 9 g/h for PM3. The drainage rate of PM1 is larger than PM2 and PM3 during the whole test. However, the drainage rates of PM2 and PM3 after stabilization show little difference, leading to minimal variation between the discharge water mass of PM2 and PM3. This phenomenon was also observed by Zhang and Hu [46]. The discharged water development feature may be attributed to the form and development of the soil column around the PHD. The soil column surrounding the PHD is a densely consolidated zone, which is formed due to vacuum pressure causing the void ratio to decrease rapidly. The small void ratio means a low permeability reducing the efficiency of drain plate. Furthermore, the discharged water mass under unit pave rate demonstrates the effect of pave rate on consolidation rate. Figure 5b indicates that the drainage rate does not increase linearly with the pave rate. This is because, as consolidation proceeds, the permeability of the treated soil decreases, causing the pave rate of PHD to no longer play a dominant role in the drainage efficiency. Therefore, although PM1 has a higher pavement rate compared to PM2 and PM3, the difference in drainage efficiency among the three tests gradually becomes smaller. Therefore, the higher supply drainage capacity cannot be fully utilized, meaning that a high pave rate is not always optimal.

3.2 Vertical/horizontal displacement (D_v/D_h) distribution

The displacement fields of clay slurry were obtained using the commercial software VIC-2D based on the DIC principle. This method involves tracking the positions of the same pixel points in two images before and after the deformation of a specimen surface to obtain the displacement vector of these pixel points, thus enabling the determination of the full-field displacement. By analyzing the

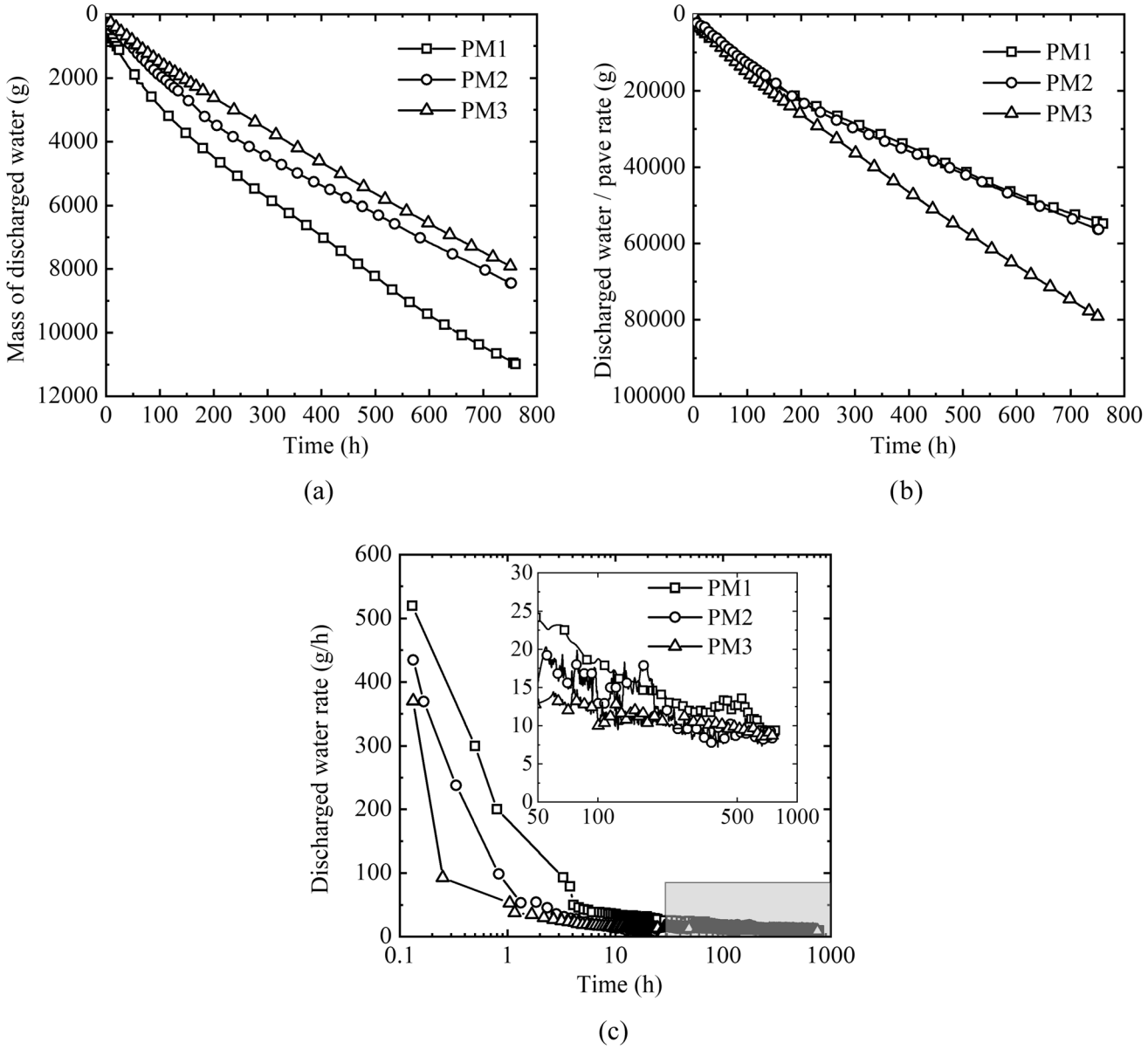

Fig. 5 Discharged water mass and water discharged rate of three PM tests: **a** mass of discharged water, **b** ratio of discharged water mass and pave rate, and **c** discharged water rate

images recorded at different moments of the consolidation test using a commercial non-contacting DIC system, the strain and displacement can be obtained. For demonstrating the reliability of the proposed new seeding method, the measured surface vertical displacements using the scale were compared with the calculated values from DIC analysis, as shown in Fig. 6. During the consolidation period of over one month, the settlement difference between scale measurement and image analysis was within 2%, indicating the enhanced DIC method was suitable for clay slurry.

Deformation information is crucial for understanding the consolidation process. Since PHD-assisted consolidation is a typical plane strain problem, vertical and horizontal displacements are equally significant. Figures. 7, 8, 9 show the displacement field distribution of the three PM tests on the 7th, 14th, and 28th day, including both vertical and horizontal directions. Analysis of displacement profiles obtained via the DIC technique reveals that the rate of vertical displacement development increases with the pave rate. Horizontal displacement in all tests with varying pave rates exhibited rapid development following the application of vacuum pressure, subsequently stabilizing. Horizontal displacement on the 7th day in the three physical model tests closely approximates that observed on the 14th and 28th days. The maximum

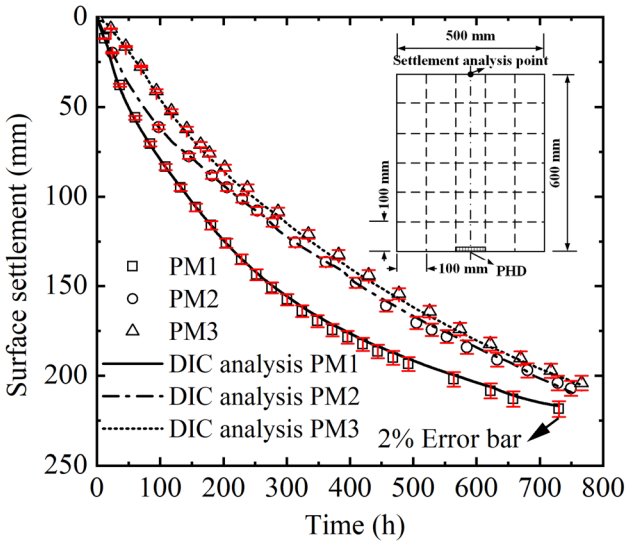

Fig. 6 Comparison between the measured surface settlement and the values from DIC analysis

horizontal displacement of the three tests is 13 mm (PM1), 12 mm (PM2), and 10 mm (PM3), which increases with the pave rate, but the difference is not large. The ratio of the maximum horizontal displacement to the maximum vertical displacement on the 28th day of the whole model tank is small, e.g., 1/17 for PM1, 1/16 for PM2, and 1/18 for PM3. Conversely, within the zone extending 10 cm from the PHD, the ratio of maximum horizontal displacement to maximum vertical displacement ranges between 1/5 and 1/4. Both the vertical and horizontal displacements close to the PHD may have a significant effect on the soil column development, a key factor in the consolidation process. Therefore, although the horizontal displacement is relatively smaller than the total displacement, its influence on the consolidation process cannot be ignored. It is noteworthy that the non-uniform surface settlement was observed according to the vertical displacement contour. After the three tests, the surface settlement showed the characteristics of being slightly larger in the middle and slightly smaller on both sides. The maximum difference in settlement amounts to approximately 10–20 mm. This phenomenon might easily be attributed solely to the boundary friction effect of the model tank. Nonetheless, observations from other model tests revealed that during the initial stage of vacuum consolidation, the trace points formed by quartz sand near the boundary remained stationary because the influence range of the drainage board did not reach both sides. Over time, the diminishment of this phenomenon occurs gradually owing to the expanding scope of influence of drainage boards. Consequently, a reasonable inference can be drawn that this phenomenon stems from non-uniform consolidation induced by PHD, as opposed to the boundary friction effect of the model tank. In addition, the settlement difference due to the non-uniform consolidation is small compared to the total settlement values. Therefore, the settlement difference has little impact on the phenomena and conclusions of the tests.

3.3 Development of soil column around PHD

To more clearly describe the directions of the soil column evolution, the drain board is divided into a permeable surface with geotextiles wrapped and cross section along the drain length. Compared with the PVD-assisted consolidation, which only provides information on the evolution of the soil column in the direction perpendicular to the permeable surface of the drain board (radial direction), the PHD-assisted consolidation model test can obtain more information on the soil column in two directions: the direction perpendicular to and parallel to the permeable surface of the drain board. The vertical displacement can be used to calculate the soil column range in the direction perpendicular to the drain board. The horizontal displacement indicates the soil column development in the direction parallel to the permeable surface of the drain board.

Displacement is a variable that accumulates over time and cannot reflect the deformation rate of the soil at specific moments. Therefore, the vertical and horizontal displacement velocities at different times were selected to analyze the soil column evolution, as displayed in Fig. 10. Observing the displacement velocity field distribution, it can be found that the dense soil column formed shortly after the application of vacuum pressure. The shape of the column is close to an ellipse which aligns with the calculated results reported by Abuel et al. [2], Huang et al. [13], and Tian et al. [35]. This ellipse soil column phenomenon is referred to as the shape effect of the band-shaped drain board. In addition, the soil column gradually became larger with time.

To determine the vertical boundary of the soil column quantitatively, Sun et al. [30] proposed defining the position with a critical displacement velocity of 0.1 mm/h (3×10^{-5} mm/s) as the soil column boundary perpendicular to the drain board based on findings from PVD-consolidation study. This method is used to determine the boundaries of vertical soil columns due to its practicality. Determining the soil column boundary parallel to the drain board is also necessary to reveal the real shape of the soil column. It has been observed that the location of maximum horizontal displacement velocity gradually shifts away from the central point of the PHD. The distance between this point and the center of the PHD approximates the major axis length of the observed soil column (as indicated in Fig. 10). Therefore, evaluating the horizontal extent of the soil column is recommended by measuring the distance from the center of the PHD to the point of maximum horizontal displacement velocity.

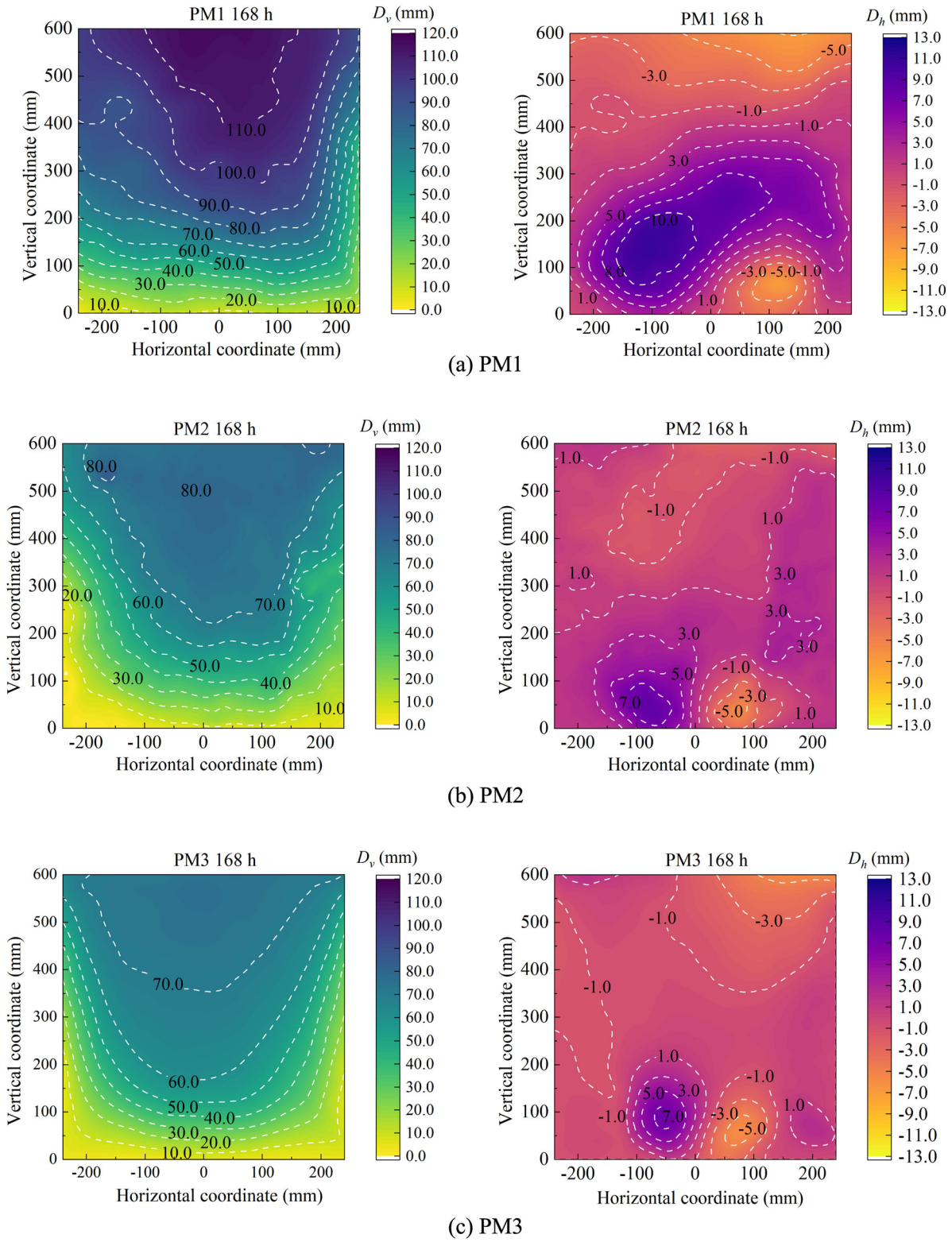

Fig. 7 Displacement field distribution 168 h after applying vacuum: **a** PM1, **b** PM2, and **c** PM3

To further verify the rationality of the findings related to the soil column evolution, the void ratio distribution was calculated based on the strain information obtained by the DIC technique. Specifically, DIC analysis provided the comprehensive plane strain data for each test, such as the vertical strain ε_y and horizontal strain ε_x. The strain

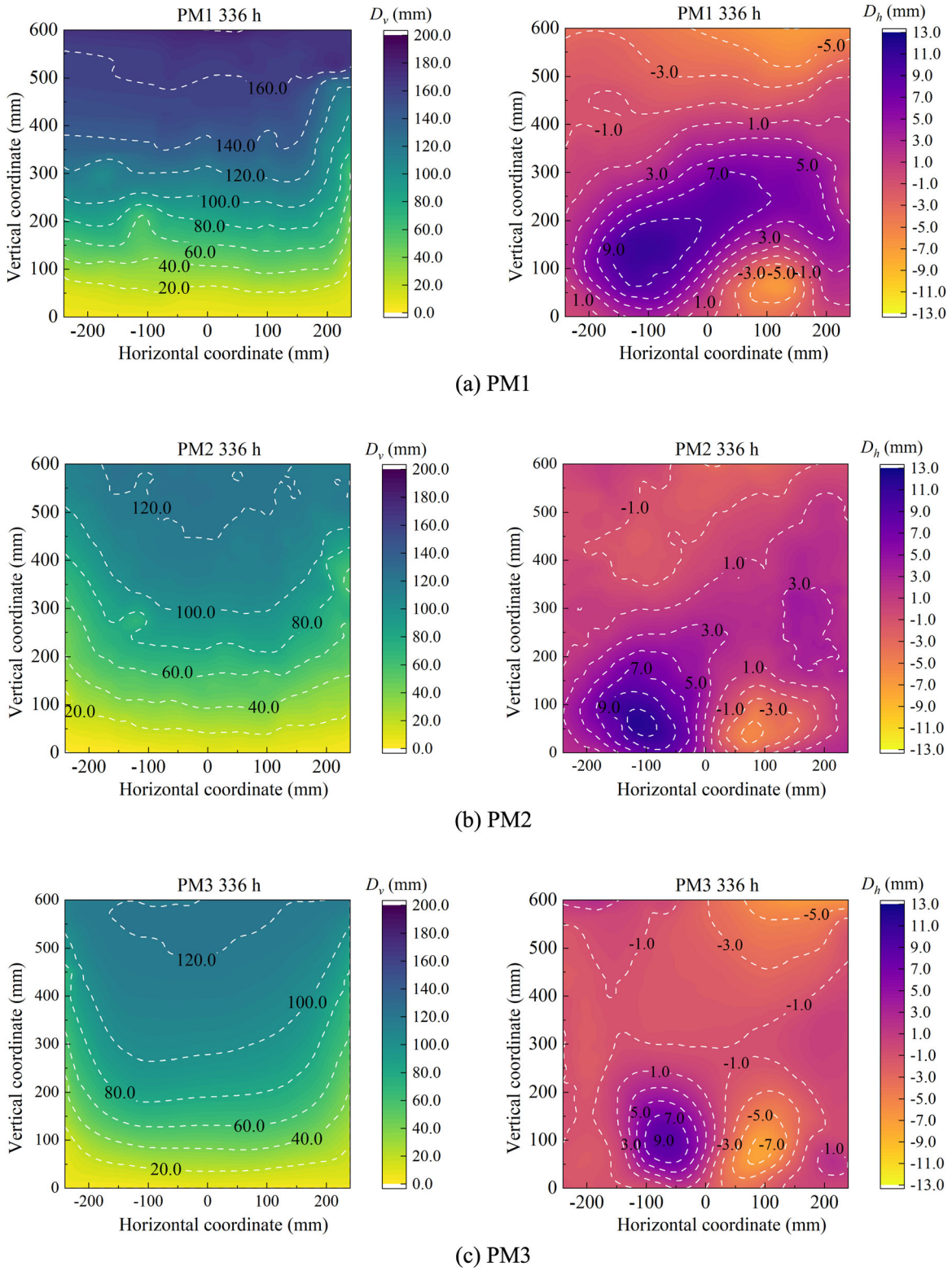

Fig. 8 Displacement field distribution 336 h after applying vacuum: **a** PM1, **b** PM2, and **c** PM3

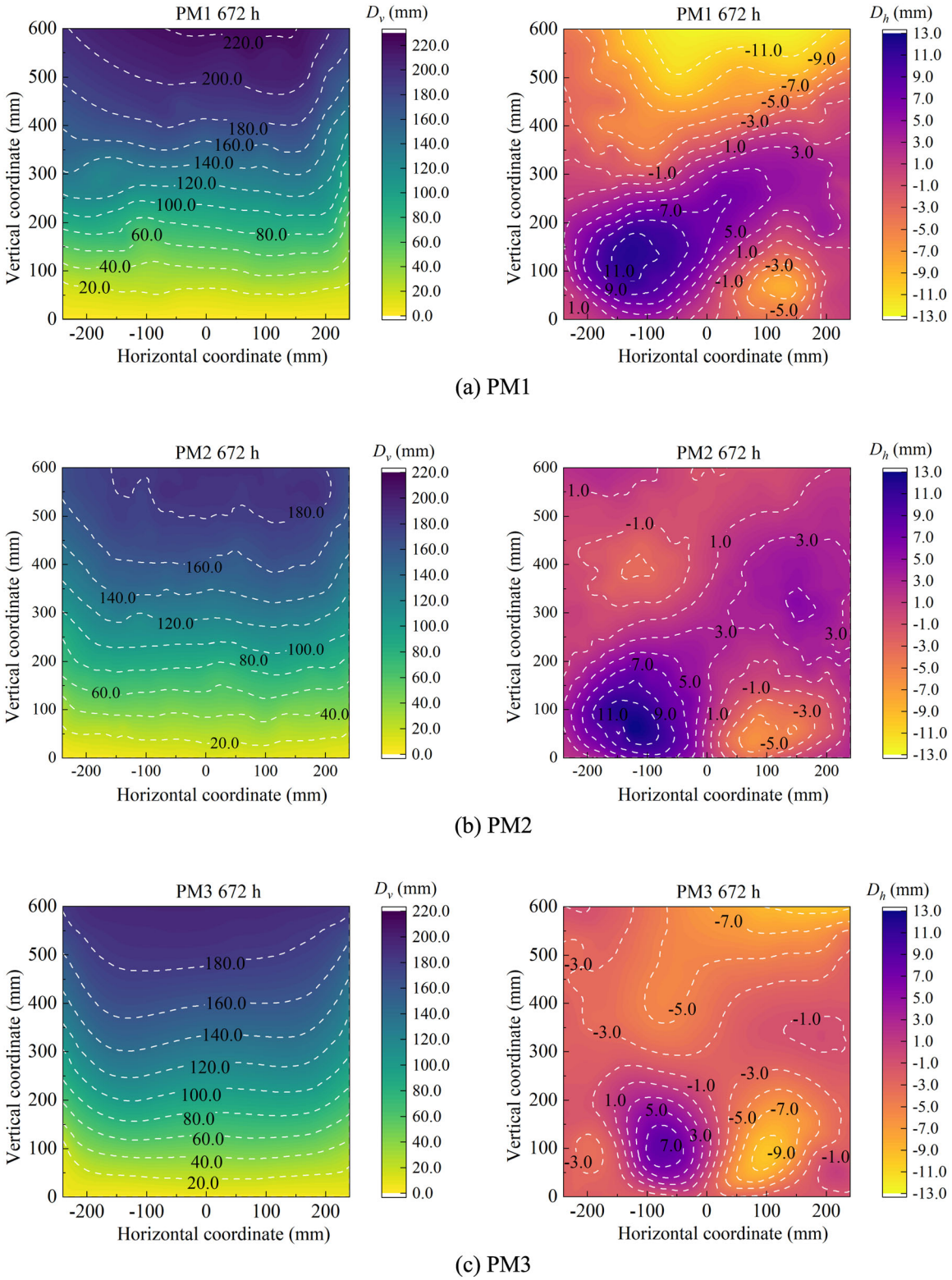

Fig. 9 Displacement field distribution 672 h after applying vacuum: **a** PM1, **b** PM2, and **c** PM3

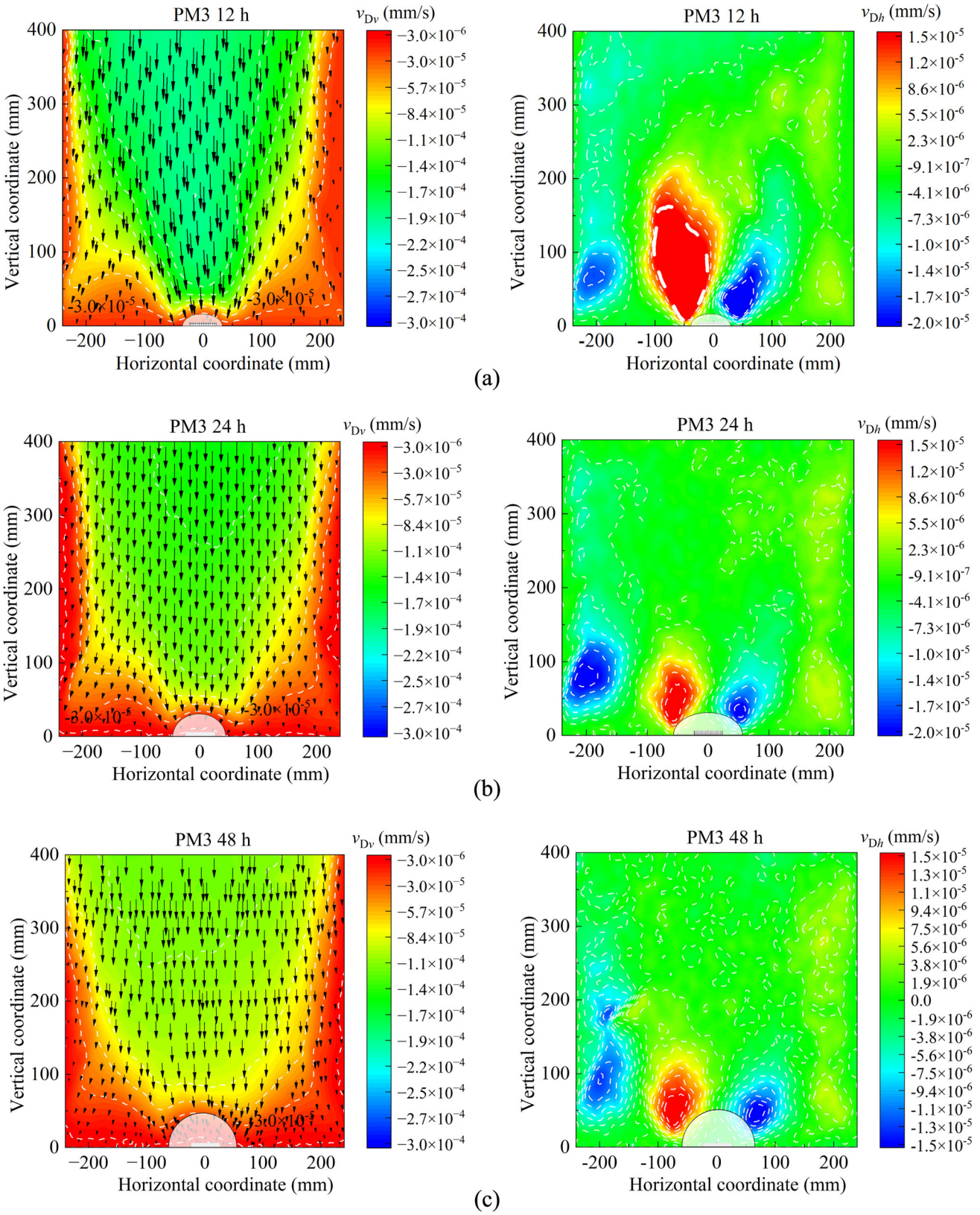

Fig. 10 Soil column development process: **a** t = 12 h, **b** t = 24 h, **c** t = 48 h, **d** t = 96 h, **e** t = 168 h, and **f** t = 336 h

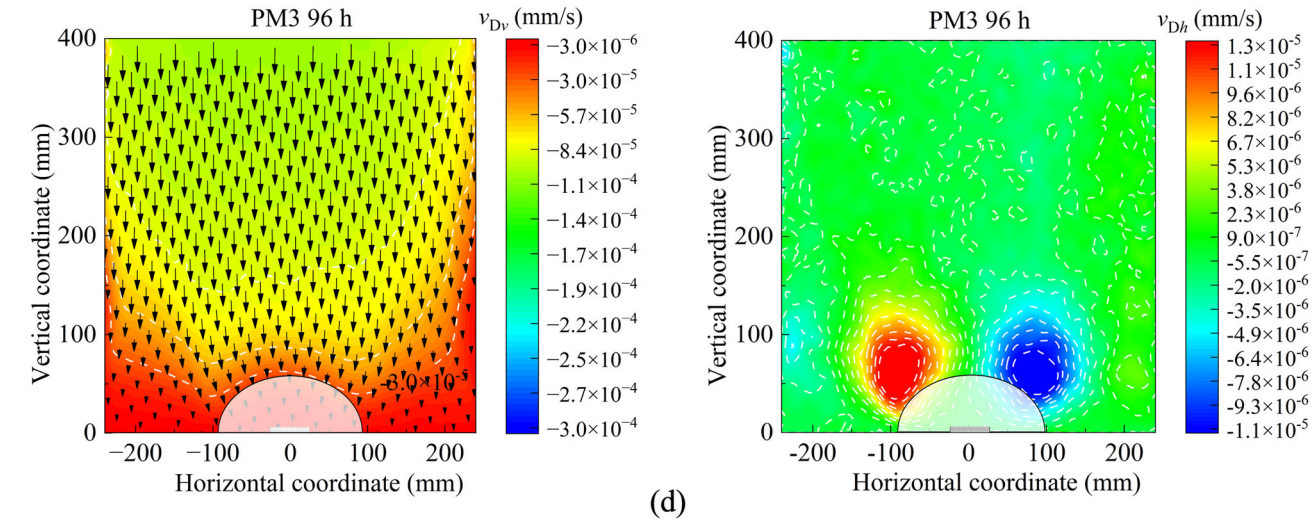

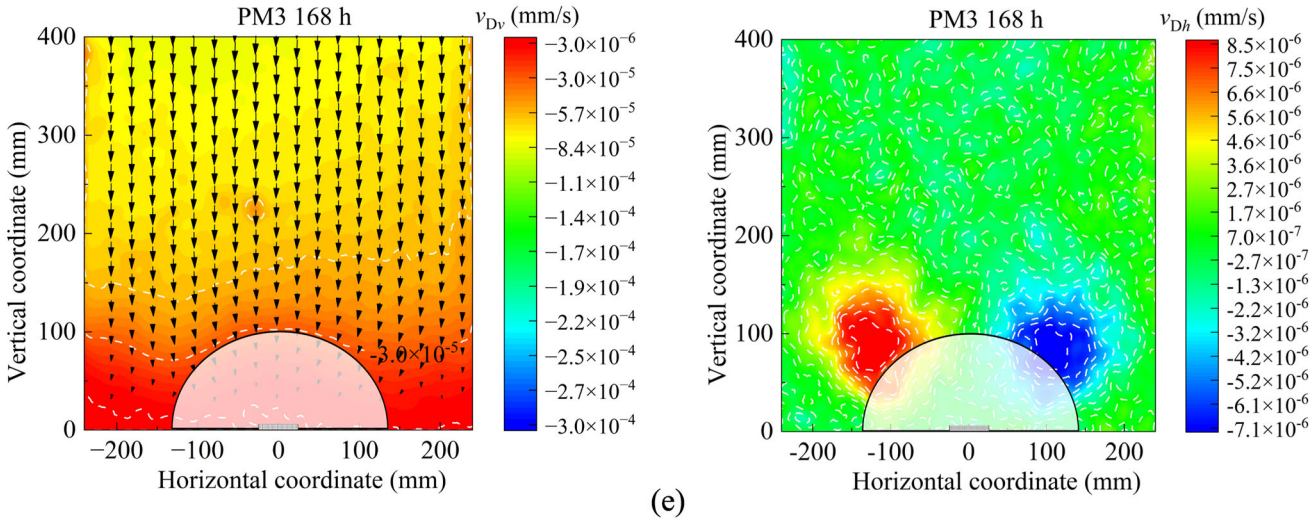

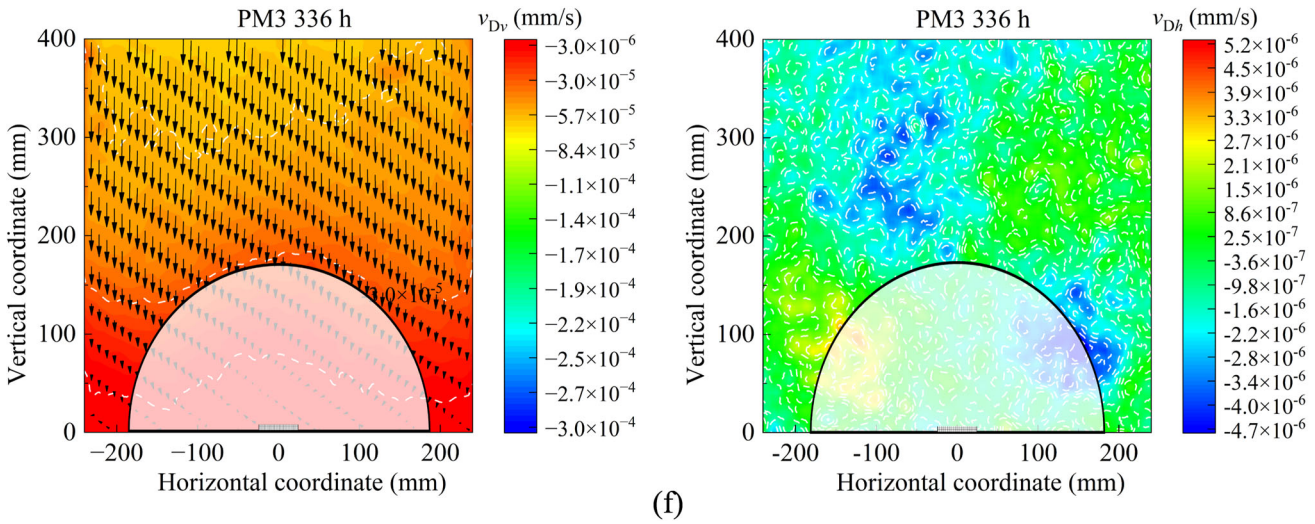

Fig. 10 continued

information can be subsequently utilized to derive the volume strain ε_V of test soil by the equation $\varepsilon_V = \varepsilon_x + \varepsilon_y$. Then by applying the relationship between void ratio e and volume strain ε_V, one can obtain the void ratio by:

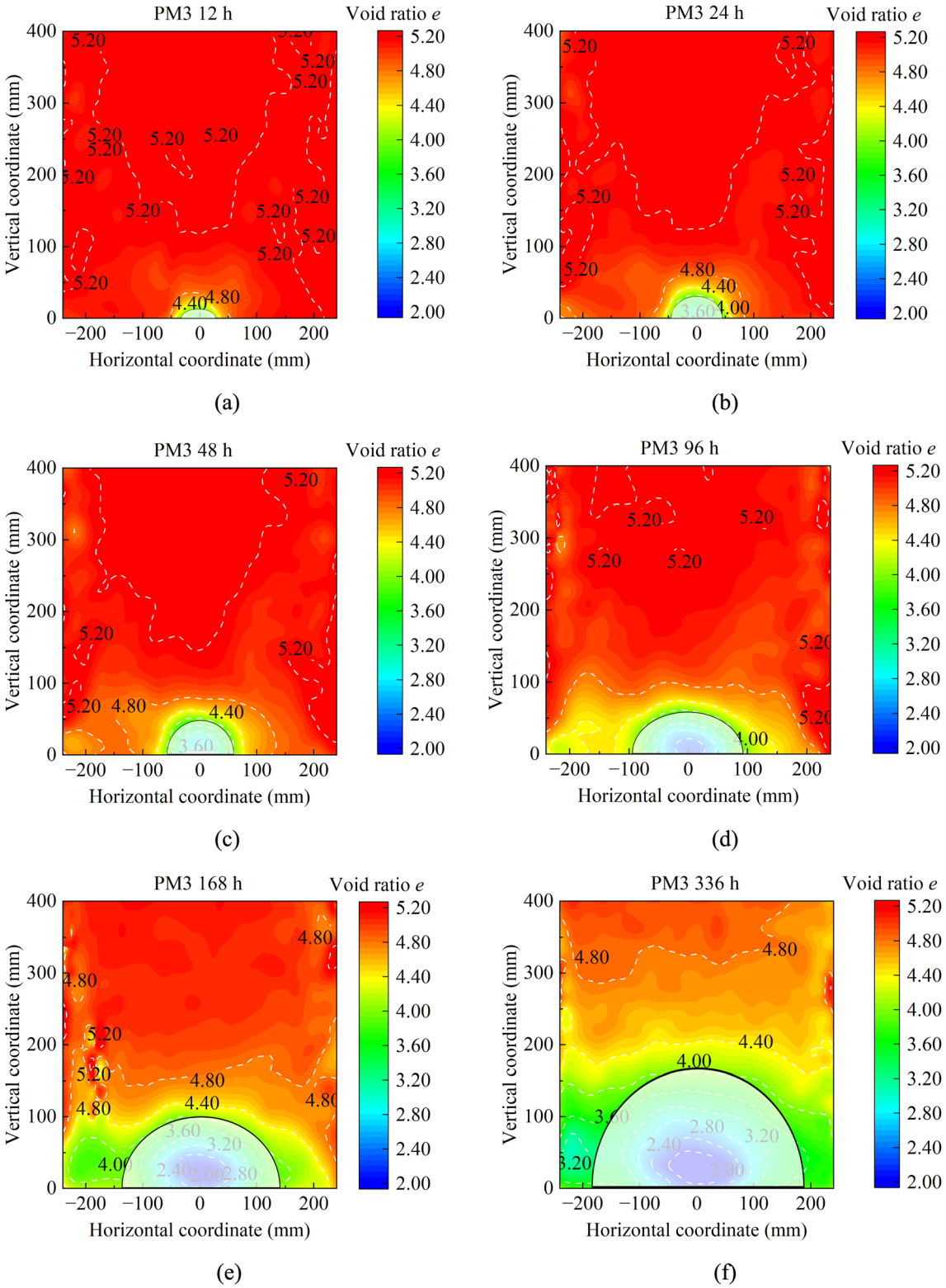

Fig. 11 Calculated void ratio distribution (PM3 test): **a** t = 12 h, **b** t = 24 h, **c** t = 48 h, **d** t = 96 h, **e** t = 168 h, and **f** t = 336 h

$$e = e_0 - (1 + e_0)\varepsilon_V \quad (1)$$

where e_0 is the initial void ratio which can be calculated by its relationship with initial water content: $e_0 = w_0 G_s$.

Figure 11 illustrates the distribution of void ratios from the PM3 test and the corresponding soil column determined through displacement velocity. Figure 11 suggests that the soil column closely aligns with the contour exhibiting a void ratio of 4. Additionally, the distribution of void ratio reveals an elliptical shape in the void ratio contour of the soil surrounding the PHD. Although the determined shape of the soil column exhibits a slight deviation from the isoline corresponding to the void ratio of 4 at 336 h, the proposed approach for determining the dimensions and configuration of soil columns is acceptable.

In summary, the vertical thickness of the observed soil column was found to conform to the equation proposed by Sun et al. [30]. Furthermore, for the horizontal thickness of soil column defining by half of the major axis of the ellipse, a fitting equation related to the width of the drain board width can be determined as follows:

$$T_{\mathrm{H}} = m(1 - \mathrm{e}^{-nt}) + W/2 \quad (2)$$

where T means the thickness, H represents the horizontal direction, m, n are fitting constants, e is the natural constant, t is the elapsed time since the vacuum preloading was applied, and W is the width of PHD. An assumption in Eq. (2) is that the initial soil column width is half of PHD width $W/2$. This assumption relies on the fact that the horizontal boundary of the observed soil column approximates the edge of the PHD in the early stages of soil column development, as shown in Figs. 10 and 11. m denotes the maximum distance from the boundary of the PHD to the horizontal boundary of the soil column.

Figure 12 displays the vertical and horizontal thickness of the soil column in three physical tests as per the previously described calculation method. Figure 12 shows that the development of the soil column progressed rapidly in both vertical and horizontal directions upon the application of vacuum loading. However, after about 100 h, the growth rate of soil column thickness began to slow down. This phenomenon is consistent with the evolution of the drainage rate. The soil column of the tests with a higher pave rate was observed to be slightly larger.

3.4 Variation in excess pore water pressure

The excess pore water pressures monitored at various positions (shown in Fig. 2) are presented in Fig. 13. Figure 13 illustrates the evolution characteristics of excess pore water pressures in the PHD-assisted consolidation tests with various pave rates. Positive excess pore pressures exist due to the self-weight stress of clay slurry at the beginning of the consolidation. The dissipation rate of excess pore water pressure increases with the PHD pave rate. The results of excess pore water pressure exhibit similarities in the three PM tests, wherein the positions closest to the PHD experience rapid and large dissipation of excess pore water pressure. Small negative pressures (e.g., approximately − 1 kPa) are recorded at position PP5 in PM1 and PM2. PP5 in PM3 exhibits almost no negative pressure due to the lowest pave rate among these three tests. Negative pressure was not found in any of the three tests at locations beyond PP5. Therefore, the effective transfer distances ranged from approximately 20 to 30 cm away from the drain board in the test duration. The excess pore water pressure distribution also suggests that the PHD can rapidly speed up the consolidation close to the PHD, while it necessitates more time for consolidation farther away from the PHD. Furthermore, the measured value at PPT 2 is similar to that at PPT 3 due to symmetrical positioning. However, variations in excess pore water pressure at PPT 1 and PPT 4 indicate potential soil non-uniformity. It should be noted that Fig. 13 demonstrates that the measured pore pressure did not converge to the applied vacuum pressure. This discrepancy is attributed to the prolonged duration required for vacuum pressure transfer, particularly due to the slow rate of transfer observed in the later stages of the test. Given that the evolution of the soil column and the characteristics of the PHD-assisted consolidation have been observed, no additional time was allocated for further vacuum transfer, thereby conserving the overall duration of the test.

3.5 Distribution of water content and undrained shear strength

The practical engineering variables of greatest concern, water content and undrained shear strength of treated soils, were also measured (as shown in Figs. 14 and 15). To avoid disturbing the soil sample, only the water content and undrained shear strength at the end of the tests were recorded. The water content was measured by slicing the soil samples into layers after the test and then using the oven-drying method. The distribution of water content in the soil revealed two distinct zones, which differed in their non-uniform characteristics along different directions. The water content of soil decreased significantly during the consolidation of the three PM tests in the zone close to the PHD, where the water content was recorded at 70% (PM1), 80% (PM2), and 80% (PM3), respectively. Similarly, the undrained shear strength was also strengthened to 12 kPa (PM1), 10 kPa (PM2), and 10 kPa (PM3) from its initial slurry state the slurry state with no strength. As such, the zone near the PHD is called the strengthened zone. The distribution of water content and undrained shear strength

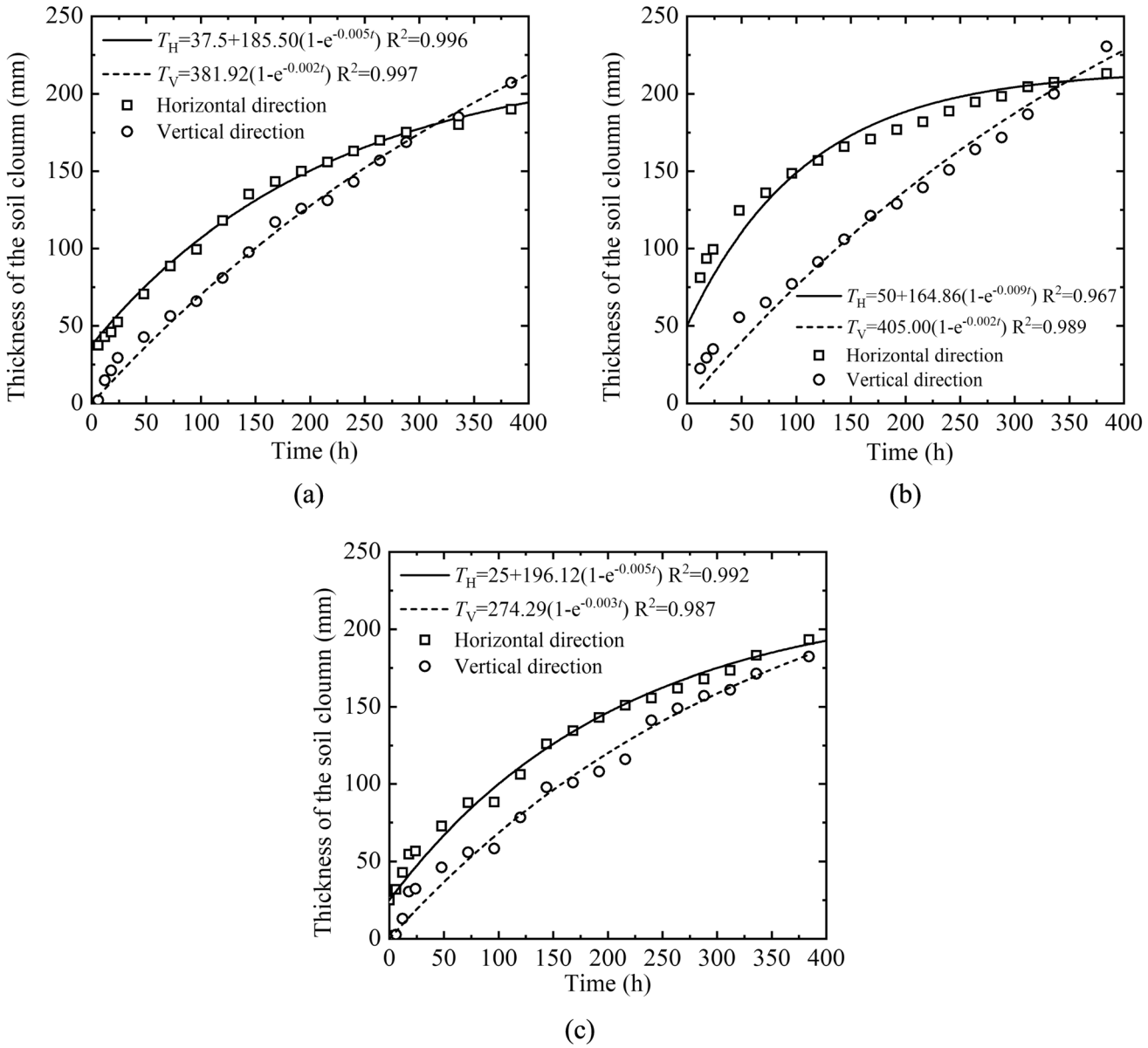

Fig. 12 Thickness of soil column obtained using DIC technique: **a** PM1; **b** PM2; and **c** PM3

in the strengthened zone appeared to the non-uniformity in both the vertical and horizontal directions. Conversely, the zone away from the PHD only displayed vertical non-uniformity. The water content and undrained shear strength have slight differences along the horizontal direction in the zone away from PHD.

Figure 16 presents a comparison between the void ratio measured in the PM3 test on the 35th day using the drying method and that obtained via the DIC technique as an example. Although a small deviation exists between the data predicted indirectly by DIC and the results obtained using the drying method, the void ratio can be generally predicted through back-calculation with DIC, both in terms of magnitude and trend. This further validates the reliability of the method for determining the void ratio based on the DIC technique. In addition, the relationship between the water content and the undrained shear strength collected from the three model tests is shown in Fig. 17. This relationship follows an exponential function $S_u = 781.72e^{-0.066w}$, with undrained shear strength decreasing as the water content increases.

3.6 Discussions

The test results demonstrate that the novel seeding method is effective in generating displacement and void ratio data for clay slurry. Compared with the existing seeding methods, the novel approach significantly enhances the

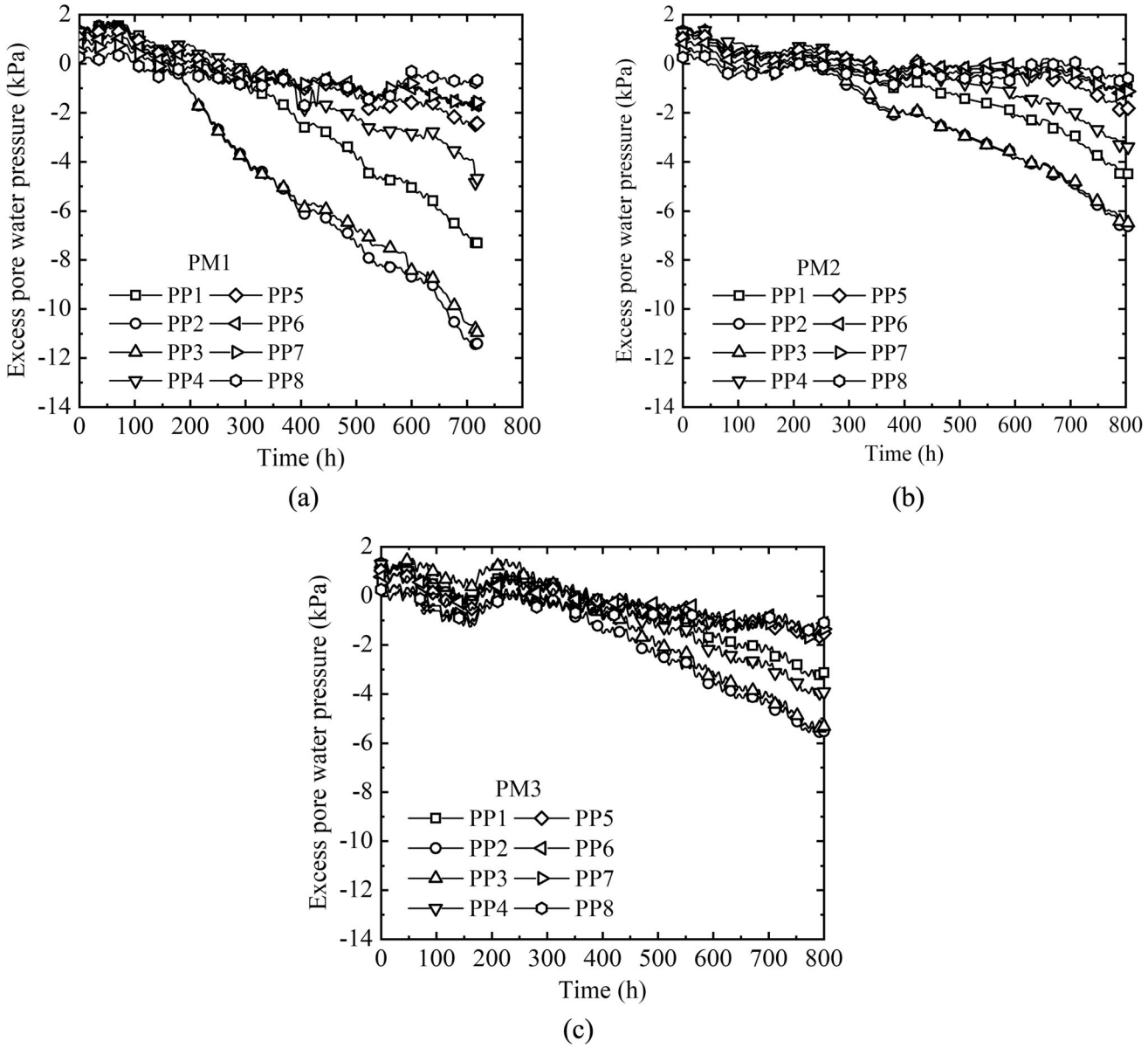

Fig. 13 Excess pore water pressure distributions at different positions: **a** PM1, **b** PM2, and **c** PM3

applicability of the DIC technique for observing the 2D strain fields in very soft soils. The discharged water data obtained from the model tests under varying pave rates experimentally suggest the existence of an optimal pave rate, a phenomenon previously only postulated in related numerical analyses. This suggests that it is unscientific to enhance the effect of accelerated consolidation merely by increasing the PHD pave rate in engineering applications. It is better to determine the optimum pave rate in engineering design. The optimal pave rate not only ensures the efficiency of PHD-accelerated consolidation but also prevents the excessive use of drain board which could lead to increased construction costs. The previous soil column studies that relied on PVD-assisted consolidation tests failed to capture the complete shape and size of the soil column. This study effectively captures the comprehensive characteristics of the soil column around the PHD through the advanced DIC technique. The test data play a critical role in deriving empirical equations that govern the determination of soil column size. The methodology for determining soil column shape provides a valuable reference for a more profound understanding of soil column formation and evolution. The empirical equations indicate the dimensions of the soil column in both the vertical and horizontal directions tend toward stable values. These values serve as valuable references for determining the optimal PHD spacing in engineering applications. However, due to the limited test data, several shortcomings

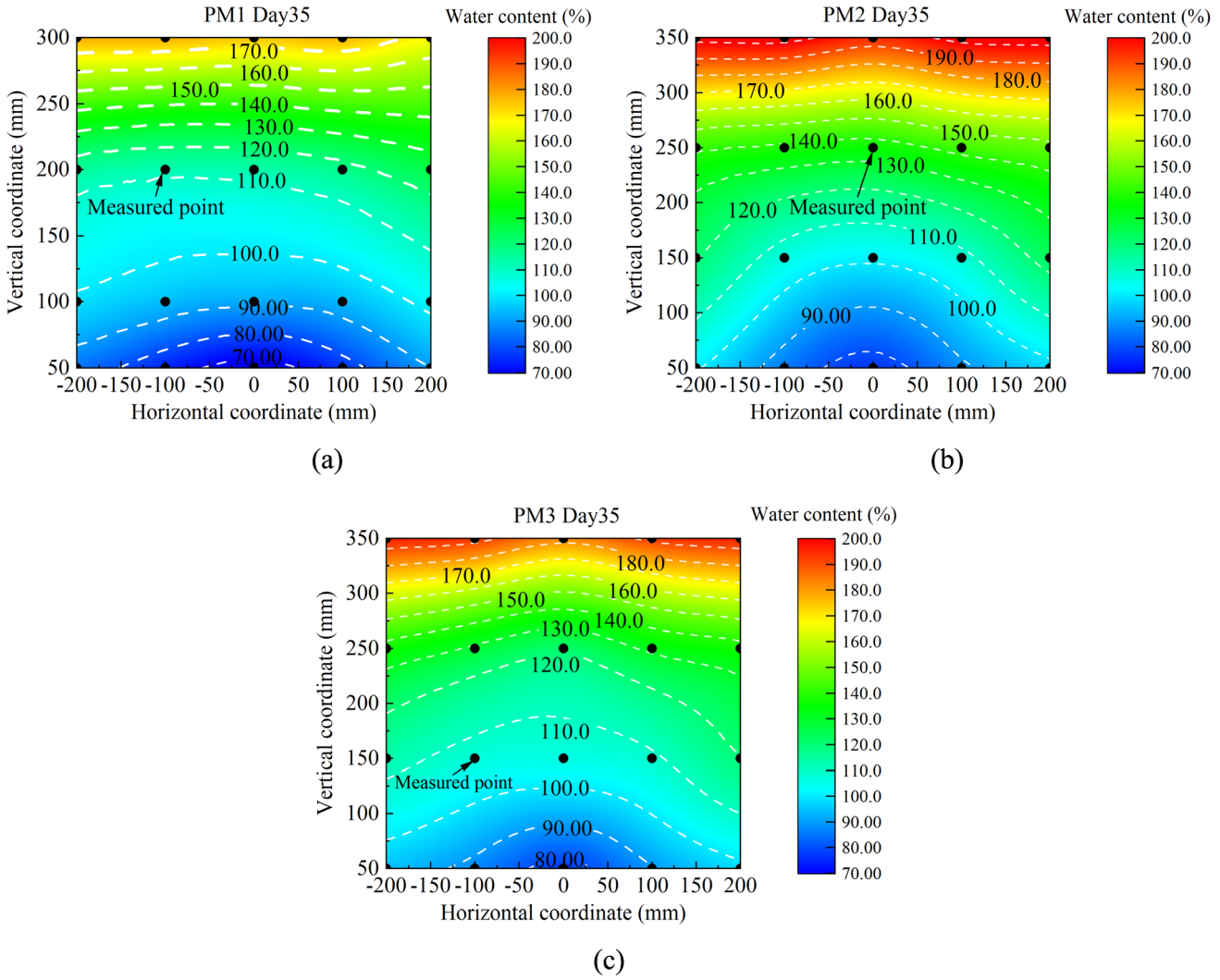

Fig. 14 Water content distributions: **a** PM1; **b** PM2; and **c** PM3

remain in this study. The methods for determining the optimal pave rate and the effective transfer distances of vacuum pressure in PHD-assisted consolidation were not provided. Although the shape and empirical equations for the evolution of soil column size were provided, its specific application method in consolidation analysis or engineering design remains unclear. Therefore, several recommendations for future work are proposed here. On the one hand, the optimal pave rate and the effective transfer distances of vacuum pressure may be influenced by numerous factors. Further investigations are recommended to quantify the optimal pave rate and the effective transfer distances of vacuum pressure in PHD-assisted consolidation, considering factors such as soil types, stress and strain states, and the duration of vacuum pressure application to the PHD. Based on the current findings and limitations of this study, future research is recommended to incorporate the observed soil column characteristics, such as shape and size, into PHD-assisted consolidation analysis to improve computational efficiency.

4 Conclusions

In summary, this study carried out several PHD-assisted consolidation model tests. The soil column evolution was observed by an enhanced DIC method, while non-uniform consolidation characteristics were systematically analyzed based on water discharge, displacement fields, pore water pressure, water content distribution, and undrained shear strength. Based on the experimental results, the following conclusions were drawn:

(a) The novel artificial seeding method can create a clear and stable texture for clay slurry, which is simple and can reduce interference from model tank installation. The DIC method based on the proposed seeding

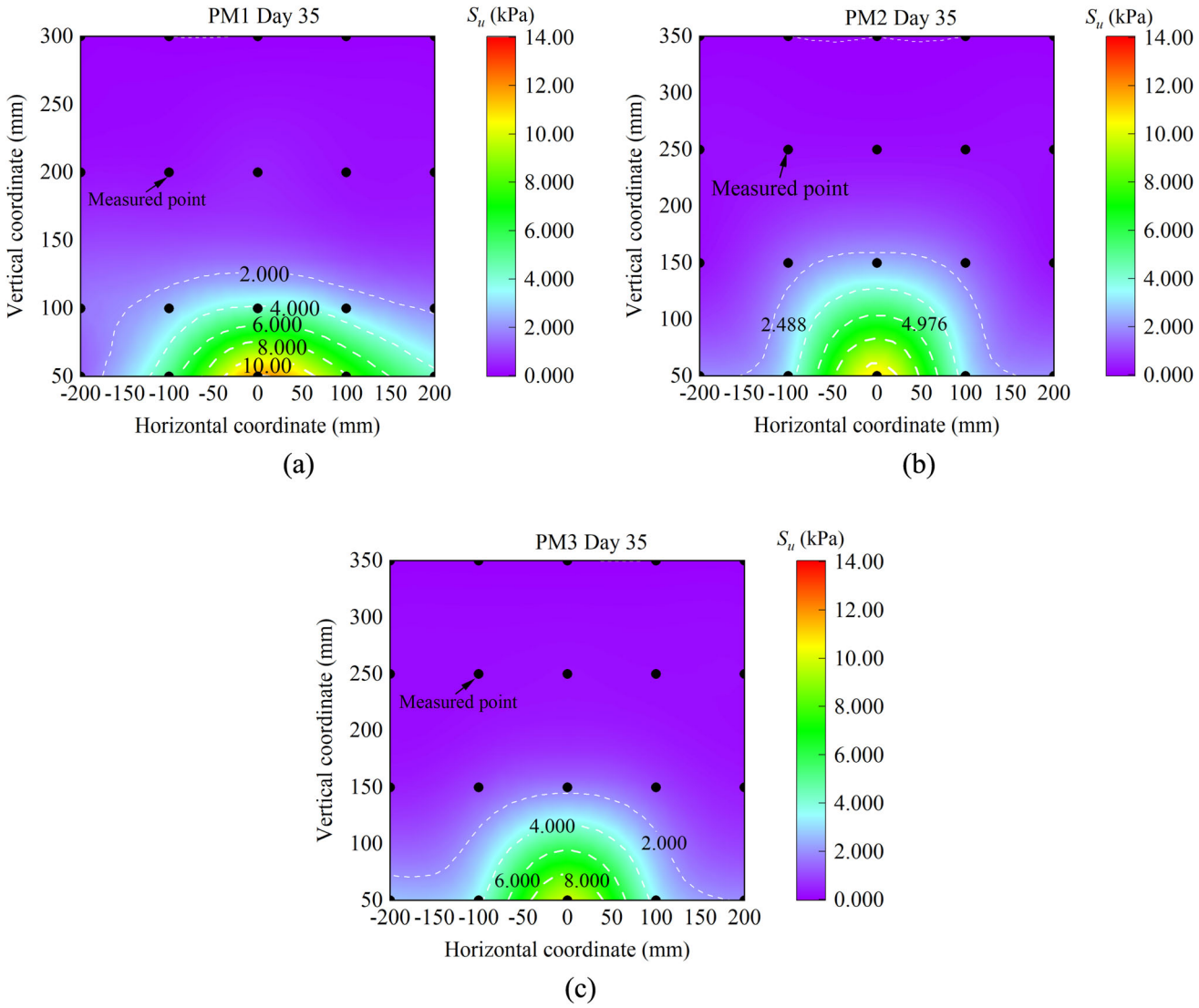

Fig. 15 Undrained shear strength distributions: **a** PM1; **b** PM2; and **c** PM3

method successfully obtained the 2D displacement field of the slurry. The displacement results, derived using both the scale and DIC methods, show excellent consistency.

(b) Higher pave rates increase discharged water mass and discharge rate, but the relationship is nonlinear. At the early stage of vacuum application, higher pave rates lead to faster water discharge. As consolidation progresses, the difference in discharge rates between tests with varying pave rates decreases. Simply increasing the pave rate is not an optimum method to enhance the PHD-accelerated effect.

(c) The plane strain displacement fields in the PHD-assisted consolidation process showed significant non-uniform characteristics. Vertical displacement developed more uniformly than horizontal displacement. Displacement near the PHD zone increased more rapidly. Horizontal displacement was concentrated near the PHD, quickly reaching its maximum and stabilizing.

(d) The shape of the soil column due to the PHD is close to an ellipse. Initially, the soil column expands rapidly when vacuum pressure is applied, but the development rate slows down later. A method to determine the soil column size using displacement velocity fields is proposed, providing insights for consolidation analysis and PHD spacing. The void ratio distribution, derived from the strain field, verifies the reliability of the findings on soil column evolution.

(e) In the PHD-assisted tests, vacuum loading effectively transfers 20-30 cm from the drain board. The pave rate significantly affects vacuum transfer efficiency. Two distinct zones are observed combining

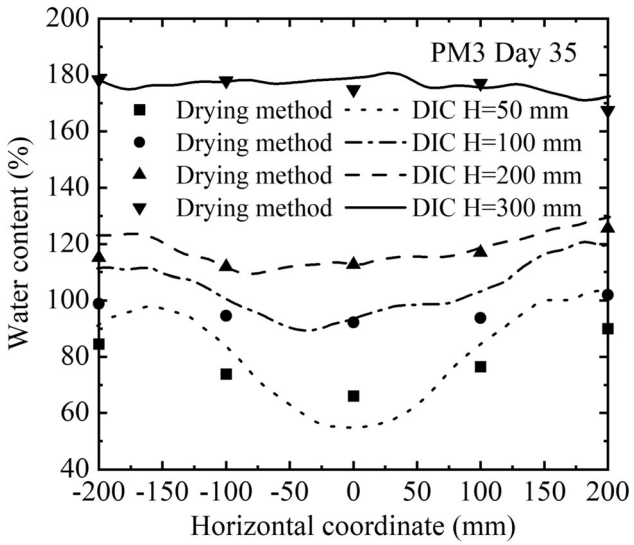

Fig. 16 Comparison between the water content of PM3 at Day 35 by drying method and DIC analysis

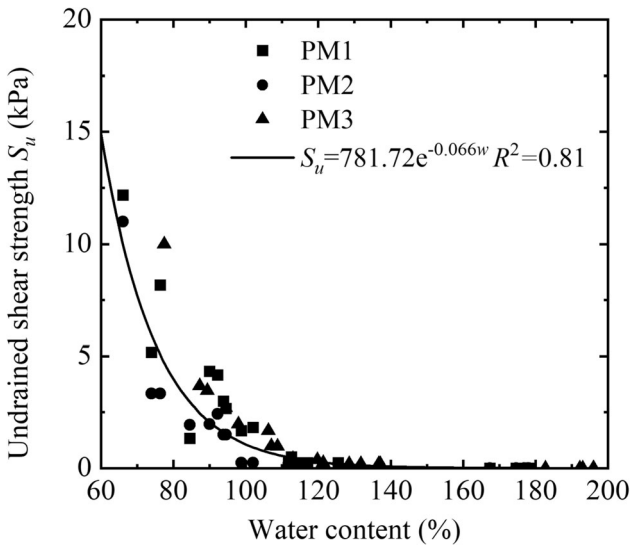

Fig. 17 Correlation between the water content and undrained shear strength

the analysis of water content and undrained shear strength distribution: the strengthened zone near the PHD, with low excess pore water pressure, low water content, and high shear strength, and a farther zone that is less affected by PHD treatment.

Supplementary Information The online version contains supplementary material available at https://doi.org/10.1007/s11440-025-02608-9.

Acknowledgements The work in this paper is supported by a Research Impact Fund (RIF) project (R5037-18), a Theme-based Research Scheme Fund (TRS) project (T22-502/18-R), the Project of RCRE (grant No.: 1-BBEM) of The Hong Kong Polytechnic University, and three General Research Fund (GRF) projects (PolyU 152179/18E; PolyU 152130/19E; PolyU 152100/20E) from Research Grants Council (RGC) of Hong Kong Special Administrative Region Government of China. The authors also acknowledge the financial supports from Research Institute for Sustainable Urban Development of The Hong Kong Polytechnic University and a grant ZDBS from The Hong Kong Polytechnic University.

Funding Open access funding provided by The Hong Kong Polytechnic University.

Data availability All data that support the findings of this study are available from the corresponding author upon reasonable request.

References

1. Abdi MR, Mirzaeifar H, Asgardun Y, Hatami K (2024) Assessment of pegged geogrid (PG) pullout performance in coarse-grained soils using PIV analysis. Geotext Geomembranes 52(1):27–45
2. Abuel-Naga HM, Bouazza A, Bergado DT (2012) Numerical assessment of equivalent diameter equations for prefabricated vertical drains. Can Geotech J 49(12):1427–1433. https://doi.org/10.1139/t2012-091
3. Cai YQ (2021) Consolidation mechanism of vacuum preloading for dredged slurry and anti-clogging method for drains. Chin J Geotech Eng 43(2):201–225
4. Chai JC, Duy QN (2013) Geocomposite induced consolidation of clayey soils under stepwise loads. Geotext Geomembranes 37:99–108. https://doi.org/10.1016/j.geotexmem.2013.02.006
5. Chai JC, Horpibulsuk S, Shen SL, Carter JP (2014) Consolidation analysis of clayey deposits under vacuum pressure with horizontal drains. Geotext Geomembranes 42(5):437–444. https://doi.org/10.1016/j.geotexmem.2014.07.001
6. Chai JC, Wang J, Ding W, Qiao Y (2022) Method for calculating horizontal drain induced non-linear and large strain degree of consolidation. Geotext Geomembranes 50(2):231–237. https://doi.org/10.1016/j.geotexmem.2021.09.008
7. Chen JF, Zhang X, Yoo C, Gu ZA (2022) Effect of basal reinforcement on performance of floating geosynthetic encased stone column-supported embankment. Geotext Geomembranes 50(4):566–580. https://doi.org/10.1016/j.geotexmem.2022.01.006
8. Chen Z, Ni PP, Chen YF, Mei GX (2020) Plane-strain consolidation theory with distributed drainage boundary. Acta Geotech 15(2):489–508. https://doi.org/10.1007/s11440-018-0712-z
9. Chen ZJ, Li PL, Li A, Yin JH, Song DB (2024) New simple method for calculating large-strain consolidation settlement of layered soft soils with horizontal drains and vacuum preloading with comparison to test data. Geotext Geomembranes 52(4):725–735

10. Chiba T, Shinsha H, Tani Y (1992) Development of a vacuum-consolidation method employing horizontal drains. Japan Dredg. Reclamat. Eng. Assoc. Tokyo (Japan).
11. Deng Y, Liu L, Cui YJ, Feng Q, Chen X, He N (2019) Colloid effect on clogging mechanism of hydraulic reclamation mud improved by vacuum preloading. Can Geotech J 56(5):611–620. https://doi.org/10.1139/cgj-2017-0635
12. He ZL, Shen MF, Yu ZY, Sun HL, Cai YQ, Yu MF, Zhang QL (2024) Effect of water content on clogging of dredged slurry under vacuum preloading from PIV perspective. Mar Georesour Geotechnol 42(6):634–646. https://doi.org/10.1080/1064119X.2023.2211979
13. Huang CX, Deng YB, Chen F (2016) Consolidation theory for prefabricated vertical drains with elliptic cylindrical assumption. Comput Geotech 77:156–166. https://doi.org/10.1016/j.compgeo.2016.04.015
14. Khachan MM, Bhatia SK (2017) The efficacy and use of small centrifuge for evaluating geotextile tube dewatering performance. Geotext Geomembranes 45(4):280–293
15. Li LH, Wang Q, Wang NX, Wang JP (2009) Vacuum dewatering and horizontal drainage blankets: a method for layered soil reclamation. Bull Eng Geol Environ 68:277–285. https://doi.org/10.1007/s10064-009-0200-7
16. Li PL, Yin ZY, Song DB, Chen ZJ, Yin JH (2025) Consolidation of clay slurry under very low stresses: from novel oedometer apparatus invention to non-linear consolidation characteristics and finite strain modelling. Can Geotech J, under review.
17. Liu FY, Li H, Wang J, Fu HT, Hu XQ, Cai Y (2024) Experimental analysis of a staged vacuum preloading method with PHD-PVD for waste slurry treatment. Acta Geotech 19(5):2487–2497
18. Menon AR, Bhasi A (2021) Numerical investigation of consolidation induced by prefabricated horizontal drains (PHD) in clayey deposits. Geotech Geol Eng 39(3):2101–2114
19. Nagahara H, Fujiyama T, Ishiguro T, Ohta H (2004) FEM analysis of high airport embankment with horizontal drains. Geotext Geomembranes 22(2):49–62. https://doi.org/10.1016/S0266-1144(03)00051-7
20. Nogami T, Li M (2003) Consolidation of clay with a system of vertical and horizontal drains. J Geotech Geoenviron Eng 129(9):838–848
21. Pan Y, Li C (2024) Installation of PHDs accelerates the self-weight consolidation of dredged sludge yards by considering the influence of the stacking process. Comput Geotech 169:106218
22. Reshma B, Viswanadham BVS, Rajagopal K (2024) Centrifuge modeling and piv analysis of geogrid reinforced pile supported embankments over soft clay. Int J Geosynth Groun 10(4):62
23. Shinsha H, Kumagai T, Miyamoto K, Hamaya T (2013) Execution for the volume reduction of dredged soil using the vacuum consolidation method with horizontal pre-fabricated drains. Geotech Eng J Jpn Geotech Soc 8(1):97–108 (**in Japanese**)
24. Song DB, Pu HF, Khoteja D, Li ZY, Yang P (2022) One-dimensional large-strain model for soft soil consolidation induced by vacuum-assisted prefabricated horizontal drain. Eur J Environ Civ Eng 26(11):5496–5516. https://doi.org/10.1080/19648189.2021.1907228
25. Song DB, Pu HF, Yin ZY, Min M, Qiu JW (2023) Plane-strain model for large strain consolidation induced by vacuum-assisted prefabricated horizontal drains. Int J Numer Anal Methods Geomech 47(10):1911–1935. https://doi.org/10.1002/nag.3544
26. Song DB, Pu HF, Yin ZY, Yin JH, Chen WB (2024) A novel analytical solution for slurry consolidation induced by a vacuum-assisted prefabricated horizontal drain. J Geotech Geoenviron Eng 150(12):04024125
27. Stanier SA, White D (2013) Improved image-based deformation measurement in the centrifuge environment. Geotech Test J 36(6):915–928. https://doi.org/10.1520/GTJ20130044
28. Stanier SA, Dijkstra J, Leśniewska D, Hambleton J, White DJ, Wood DM (2016) Vermiculate artefacts in image analysis of granular materials. Comput Geotech 72:100–113. https://doi.org/10.1016/j.compgeo.2015.11.013
29. Stanier SA, Blaber J, Take WA, White DJ (2016) Improved image-based deformation measurement for geotechnical applications. Can Geotech J 53(5):727–739. https://doi.org/10.1139/cgj-2015-0253
30. Sun HL, He ZL, Geng XY, Shen MF, Cai YQ, Wu J, Yang B, Wang WJ (2022) Formation mechanism of clogging of dredge slurry under vacuum preloading visualized using digital image technology. Can Geotech J 59(7):1292–1298. https://doi.org/10.1139/cgj-2021-0341
31. Sun HL, He ZL, Pan K, Lu JL, Pan XD, Shi L, Geng XY (2022) Consolidation mechanism of high-water-content slurry during vacuum preloading with prefabricated vertical drains. Can Geotech J 59(8):1373–1385. https://doi.org/10.1139/cgj-2021-0248
32. Sun HL, Zhang H, Geng XY, Cui YJ, Cai YQ (2023) Large-strain consolidation analysis for clayey sludge improved by horizontal drains. J Geotech Geoenviron Eng 149(8):04023057. https://doi.org/10.1061/JGGEFK.GTENG-11511
33. Take WA (2015) Thirty-sixth Canadian Geotechnical Colloquium: advances in visualization of geotechnical processes through digital image correlation. Can Geotech J 52(9):1199–1220. https://doi.org/10.1139/cgj-2014-0080
34. Teng Y, Stanier SA, Gourvenec SM (2017) Synchronised multi-scale image analysis of soil deformations. Int J Phys Model Geotech 17(1):53–71. https://doi.org/10.1680/jphmg.15.00058
35. Tian Y, Jiang GS, Wu WB, Wen MJ, Zhang ZT, El Naggar MH, Mei GX, Dong YK (2021) Elliptical cylindrical equivalent model of PVD-assisted consolidation under surcharge combined with vacuum preloading and its application. Comput Geotech 139:104389. https://doi.org/10.1016/j.compgeo.2021.104389
36. Wang P, Han YB, Zhou Y, Wang J, Cai YQ, Xu F, Pu HF (2020) Apparent clogging effect in vacuum-induced consolidation of dredged soil with prefabricated vertical drains. Geotext Geomembranes 48(4):524–531. https://doi.org/10.1016/j.geotexmem.2020.02.010
37. Wang P, Wu JF, Ge XY, Chen F, Yang XT (2022) Non-uniform consolidation of soil and influence of corresponding clogging effect during vacuum preloading. Int J Geosynth Groun 8(5):58. https://doi.org/10.1007/s40891-022-00402-1
38. White DJ, Take WA, Bolton MD (2003) Soil deformation measurement using particle image velocimetry (PIV) and photogrammetry. Géotechnique 53(7):619–631. https://doi.org/10.1680/geot.2003.53.7.619
39. Wu JQ, Ouyang CL, Dai M, Gao ZY, Fu HT, Wang J (2023) Effect of surcharge loading rate on the performance of surcharge-vacuum preloading with prefabricated horizontal drains. Mar Georesour Geotechnol 41(7):806–814. https://doi.org/10.1080/1064119X.2022.2101964
40. Wu YJ, Li JP, Lu YT, Zhang XD, Le TH, Chau NXQ (2021) The influence of drainage spacing on the deformation characteristics of transparent ultrasoft soil. Int J Geosynth Groun 7(4):99. https://doi.org/10.1007/s40891-021-00343-1
41. Xu BH, He N, Jiang YB, Zhou YZ, Zhan XJ (2020) Experimental study on the clogging effect of dredged fill surrounding the PVD under vacuum preloading. Geotext Geomembranes 48(5):614–624. https://doi.org/10.1016/j.geotexmem.2020.03.007
42. Yang K, Lu M, Sun J, Liu G (2024) Experimental study on dewatering and reinforcement of dredged slurry treated by PHDs-PVDs under step vacuum preloading. Geotext Geomembranes 52(5):887–899

43. Yin JH, Chen WB, Leung AYF (2023) A sustainable approach to marine reclamations and a field trial at Tung Chung New Town Extension Site in Hong Kong.
44. Zhang H, Sun HL, Liu SJ, Chu J, Shi L, Geng XY, Deng YF, Cai YQ (2023) Large-strain consolidation of sludge in multiple-drainage geotextile tubes. J Geotech Geoenviron Eng 149(6):04023037. https://doi.org/10.1061/JGGEFK.GTENG-1118
45. Zhang H, Wang WJ, Liu SJ, Chu J, Sun HL, Geng XY, Cai YQ (2022) Consolidation of sludge dewatered in geotextile tubes under combined fill and vacuum preloading. J Geotech Geoenviron Eng 148(6):04022032. https://doi.org/10.1061/(ASCE)GT.1943-5606.0002791
46. Zhang L, Hu L (2019) Laboratory tests of electro-osmotic consolidation combined with vacuum preloading on kaolinite using electrokinetic geosynthetics. Geotext Geomembranes 47(2):166–176. https://doi.org/10.1016/j.geotexmem.2018.12.010
47. Zhang X, Rajesh S, Chen JF, Wang JQ (2022) Geosynthetic encased column-supported embankment: behavior with and without basal geogrid. Geosynth Int 29(3):312–325. https://doi.org/10.1680/jgein.21.00038
48. Zhou Y, Chai JC (2017) Equivalent 'smear' effect due to non-uniform consolidation surrounding a PVD. Géotechnique 67(5):410–419. https://doi.org/10.1680/jgeot.16.P.087
49. Zhou Y, Yang H, Wang P, Yang XT, Xu F (2022) Vacuum-induced lateral deformation around a vertical drain in dredged slurry. Geosynth Int 29(5):495–505. https://doi.org/10.1680/jgein.21.00006a
50. Zhou Y, Yin B, Wang P, Ge X, Zhao B (2024) Pilot test and consolidation theory of marine dredged slurry using the membrane-free horizontal-vacuum method. Ocean Eng 293:116650